



InSAR mapping and geophysical investigation of ground deformations in Tanjung Bungah, Penang Island, Malaysia

Kazeem Olukunle Rauff^{1,2} · Ismail Ahmad Abir¹ · Daniel Perissin³

Received: 1 March 2021 / Accepted: 12 August 2022 / Published online: 18 August 2022
© Saudi Society for Geosciences 2022

Abstract

Detailed research was carried out on Penang Island's ground deformation due to the region's high reflectivity and ground displacement potential. A combined remote sensing technique and geophysical survey were applied. Fifty-six descending Sentinel-1A (S-1A) Synthetic Aperture Radar (SAR) data were processed by the Permanent Scatterer Interferometric Synthetic Aperture Radar (PS-InSAR) technique in SARPROZ software to detect, calculate, and map ground deformation patterns in the area. A geophysical survey was also performed using the Ground Penetrating Radar (GPR) method to investigate subsurface activities based on InSAR results. Although the entire Penang Island's ground deformation was mapped, the analyses were limited to one of the ground deformation areas, namely Tanjung Bungah. The area is a high-risk landslide zone due to its incohesive soil composition. Ground deformation significantly affects the lives and properties of the people of the area. InSAR result indicates an active ground movement (subsidence) of around -10 mm/yr. The value of 5.00 mm/yr for the uplift pattern was also observed. The detected GPR anomalies (cavities, fractures, and road fissures) correspond to the subsidence PS points. InSAR and geophysical data have a strong association with subsurface disturbances.

Keywords PS-InSAR · Landslide · Subsidence · SPSS · Sentinel-1A · Geophysical surveys

Introduction

The population growth leads to the exploitation of land for development (rail, road constructions, and building of infrastructure). These facilities and other modern amenities are located in hazardous areas on Penang Island, Malaysia, because of limited flatlands, necessitating the region's expansion to compensate for growth (Rauff et al. 2020). The Penang state government allows buildings on hill slopes that are not exceeding 25° in gradient and 76 m above sea level (asl) due to the shortage of flatlands. However, most

developers circumvent the government restrictions but get approval on natural slopes, which are quite different from the stipulated threshold. Most of the region's constructed roads and high-rise buildings involve hill cutting, land reclamation, and deforestation. These activities, particularly during the rainy season, have led to various ground deformations (e.g., slope failures, sinkhole, landslides, subsidence, etc.), claimed many lives, and damaged multiple properties (Rocca et al. 2003, 2014; Ali et al. 2011; Rauff et al. 2020).

Recently, in Tanjung Bungah, Penang Island, the recorded cases of ground deformation have increased dramatically and affected the lives and properties of people living in the area (Thuro et al. 2010; Pradhan et al. 2014). The soil in the area is composed mainly of incohesive granite rocks that are quickly eroded and prone to landslides, resulting in slope instability (Rauff et al. 2020). An excellent example of landslide incidence was the Lengkok Lembah Permai, Tanjung Bungah landslide event in 2017, as depicted in Fig. 1a. Eleven people were buried alive after a natural slope of 18° in gradient was cut back to a 67° slope that led to ground instability 2017 (Chacko 2019). Another incidence was a collapsed retaining wall protecting the road at a newly completed housing area built on a hillslope, a water

Responsible Editor: Narasimman Sundararajan

✉ Kazeem Olukunle Rauff
olukunleid@gmail.com

¹ School of Physics, Universiti Sains Malaysia,
11800 Penang Island, Malaysia

² Department of Physics, Federal University of Kashere,
P.M.B. 0182, Gombe, Nigeria

³ School of Civil Engineering, Purdue University, 550 Stadium
Mall Drive Office: HAMP 4106, West Lafayette, IN 47907,
USA

Fig. 1 Field photographs showing various ground deformations: (a) depicts a landslide scar on 67° slopes at Tanjung Bungah, (b) represents a collapsed retaining wall protecting the road at a newly completed housing area built on a hillslope, at Tanjung Bungah, (c) shows subsidence event in Mount Erskine, near Tanjung Bungah (Chacko 2019), and (d) denotes photograph of the slide area overlaid to a Google Earth image



catchment area along Jalan Persiaran, Tanjung Bungah in 2017, as shown in Fig. 1b. The soil became soft and unable to sustain the concrete barrier due to heavy and persistent rainfall. Another example of ground deformation in the area was the subsidence and sinkhole events in Mount Erskine, near Tanjung Bungah in 2017, as presented in Fig. 1c, where many families lost their houses to heavy rain that lasted for several hours. The rain caused the soil to lose its cohesion and sink, which weakened the structural strength of some buildings. The photography of the landslide area in Tanjung Bungah is shown in Fig. 1d.

There is a need for the government and local planning authorities to take this phenomenon into account at all stages by creating greater awareness of the hazard for safety planning as it brings significant challenges to the environment, particularly on unstable slope areas. The ground movement needs consistent and continuous studying and monitoring to mitigate natural hazards (Perissin and Wang 2012). Choosing the most suitable, low-cost, time-efficient, and accurate method is essential to determine the hazard. Several approaches (Guzzetti et al. 1999; Van Westen 2000; Lee and Pradhan 2006; Pradhan and Lee 2010; Oh and Pradhan 2011; Kavzoglu et al. 2014; Huang et al. 2020) have been introduced worldwide in different areas to monitor and map ground deformations, as each method has its attributes (Thuro et al. 2010; Bayer et al. 2017). The previous studies of ground deformation in Penang Island were based on applying GIS and Landsat imagery to assess landslide risk (Tan et al. 2010; Pradhan et al. 2012), artificial neural network modellings (Pradhan and Lee 2010; Gazzaz et al. 2012), and probabilistic simulations (Galve et al. 2015).

They also evaluated landslide and subsidence hazards using GIS, fuzzy logic (Choi et al. 2010). None of the highlighted studies on the most prominent ground deformation in Penang Island quantified this hazard. However, most methods and models successfully tackled engineering and environmental issues in the area. Therefore, it is essential to know the displacement rate of ground deformation to ensure grounds are indeed stabilised and worth living on. It is also essential to validate the results using the geophysical method.

Remote sensing data are widely used to detect and monitor ground deformation (Tofani et al. 2013; Tymchenko et al. 2016). Field surveys are also applied for ground deformation identification and characterisation because they are useful for investigations at the local scale and known deformation areas. However, the GPR method is used in this article. Remote sensing and geophysical techniques are combined to detect, analyse, and map ground deformation patterns in Tanjung Bungah, Penang Island.

Geology and area of study

Penang Island is in the northwest of Peninsular Malaysia (Fig. 2a). Its soil sequence is classified as granitic soil formed by an un-transported deposition of organic material and grouped into eight forms (Tan 1994; Ahmad et al. 2014), as presented in Table 1. It has a geographical coordinate that lies between the longitudes (5° 8' N–5° 35' N) and latitudes (100° 8' E–100° 32' E) (Fig. 2b) with an area size of approximately 300 km² and an estimated population of 720,000 people. The area's elevation ranges from 0 to 420 m

Fig. 2 Map of Peninsular Malaysia (a), geographical location and geological map of Penang Island city (b), and map of the study area: Tanjung Bungah (c)

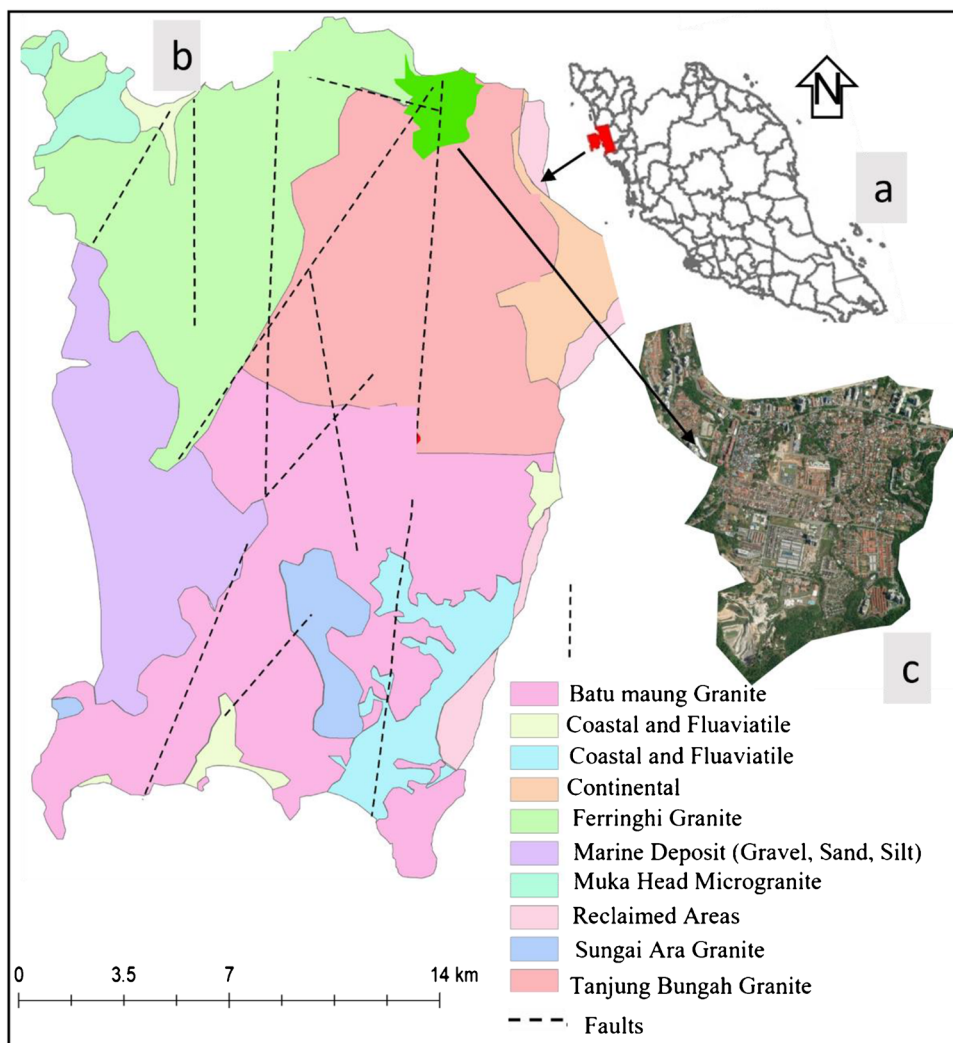


Table 1 Series of soils of Pulau Pinang (Pradhan and Lee 2010)

Series of soil	Size of grain	Texture
Steep land	Fine to medium	Clay
Urban land	Fine to medium	Sand and gravel
Serong	Medium to coarse	Clay
Rengam	Fine to medium	Coarse sandy-clay
Local alluvium-colluvium Association	Fine grain	Loam
Kuala-Kedah Permatang Association	Medium to coarse	Clay
Selangor-Kangkong Association	Medium	Clay
Rengam Bukit Temian Association	Medium to coarse	Loam

asl, with the slope varying between 25° and 87° in gradient (Pradhan et al. 2012).

The high reflectivity (due to ground cover by tall buildings and constructions along the hills), different topography (high elevated hills in the centre and flat areas to the east and west), ground displacement potential, and the abundance of previously performed geotechnical studies make the research area credible. Tanjung Bungah (whose map is depicted in

Fig. 2c) is an area of tourism located on the north coast of Penang Island with a relatively plain topography. The area is situated at the coordinate of 5° 27' 37.76" N and 100° 16' 50.49".

The core north of Penang Island (Tanjung Bungah), where significant reports of landslide events are recorded, is covered by the steep soil (Ali et al. 2011). Its grain size contains fine to coarse-grained biotite granite with orthoclase

Table 2 Descending S-1A dataset (master image is stressed in yellow colour)

Date	Pass	Polarisation	Path	Frame	Mode	Normal baseline	Temporal baseline
2017/01/09	Descending	VV + VH	164	575	IW	56	-1354
2017/01/21	Descending	VV + VH	164	575	IW	-4	-997
2017/02/02	Descending	VV + VH	164	575	IW	34	-985
2017/02/14	Descending	VV + VH	164	575	IW	76	-913
2017/02/26	Descending	VV + VH	164	575	IW	31	-961
2017/03/10	Descending	VV + VH	164	575	IW	36	-949
2017/03/22	Descending	VV + VH	164	575	IW	-39	-937
2017/04/03	Descending	VV + VH	164	575	IW	25	-925
2017/04/15	Descending	VV + VH	164	575	IW	76	-913
2017/04/27	Descending	VV + VH	164	575	IW	3	-901
2017/05/09	Descending	VV + VH	164	575	IW	112	-889
2017/05/21	Descending	VV + VH	164	575	IW	58	-877
2017/06/02	Descending	VV + VH	164	575	IW	31	-865
2017/06/14	Descending	VV + VH	164	575	IW	-4	-853
2017/06/26	Descending	VV + VH	164	575	IW	36	-841
2017/07/20	Descending	VV + VH	164	575	IW	-3	-817
2017/08/01	Descending	VV + VH	164	575	IW	65	-805
2017/09/06	Descending	VV + VH	164	575	IW	-10	-769
2017/09/18	Descending	VV + VH	164	575	IW	67	-757
2017/09/30	Descending	VV + VH	164	575	IW	64	-745
2017/10/12	Descending	VV + VH	164	575	IW	74	-733
2017/10/24	Descending	VV + VH	164	575	IW	87	-721
2017/11/05	Descending	VV + VH	164	575	IW	47	-709
2017/11/17	Descending	VV + VH	164	575	IW	38	-697
2017/11/29	Descending	VV + VH	164	575	IW	14	-685
2017/12/11	Descending	VV + VH	164	575	IW	-3	-673
2017/12/23	Descending	VV + VH	164	575	IW	-22	-661
2018/01/04	Descending	VV + VH	164	575	IW	19	-649
2018/01/16	Descending	VV + VH	164	575	IW	58	-637
2018/01/28	Descending	VV + VH	164	575	IW	7	-625
2018/03/17	Descending	VV + VH	164	575	IW	32	-577
2018/03/29	Descending	VV + VH	164	575	IW	0	0
2018/04/10	Descending	VV + VH	164	575	IW	12	-553
2018/04/22	Descending	VV + VH	164	575	IW	25	-541
2018/05/04	Descending	VV + VH	164	575	IW	-3	-529
2018/05/16	Descending	VV + VH	164	575	IW	40	-517
2018/05/28	Descending	VV + VH	164	575	IW	26	-505
2018/06/09	Descending	VV + VH	164	575	IW	45	-493
2018/06/21	Descending	VV + VH	164	575	IW	13	-481
2018/07/03	Descending	VV + VH	164	575	IW	-67	-469
2018/07/15	Descending	VV + VH	164	575	IW	9	-457
2018/07/27	Descending	VV + VH	164	575	IW	7	-445
2018/08/08	Descending	VV + VH	164	575	IW	13	-433
2018/08/20	Descending	VV + VH	164	575	IW	0	-421
2018/09/01	Descending	VV + VH	164	575	IW	88	-409
2018/09/13	Descending	VV + VH	164	575	IW	15	-397
2018/09/25	Descending	VV + VH	164	575	IW	0	-385
2018/10/07	Descending	VV + VH	164	575	IW	8	-373
2018/10/19	Descending	VV + VH	164	575	IW	68	-361
2018/10/31	Descending	VV + VH	164	575	IW	79	-349
2018/11/12	Descending	VV + VH	164	575	IW	83	-337

Table 2 (continued)

Date	Pass	Polarisation	Path	Frame	Mode	Normal baseline	Temporal baseline
2018/11/24	Descending	VV + VH	164	575	IW	27	- 325
2018/12/06	Descending	VV + VH	164	575	IW	86	- 313
2018/12/18	Descending	VV + VH	164	575	IW	- 34	- 301
2018/12/30	Descending	VV + VH	164	575	IW	47	- 289

Fig. 3 Flowchart for S-1A data processing

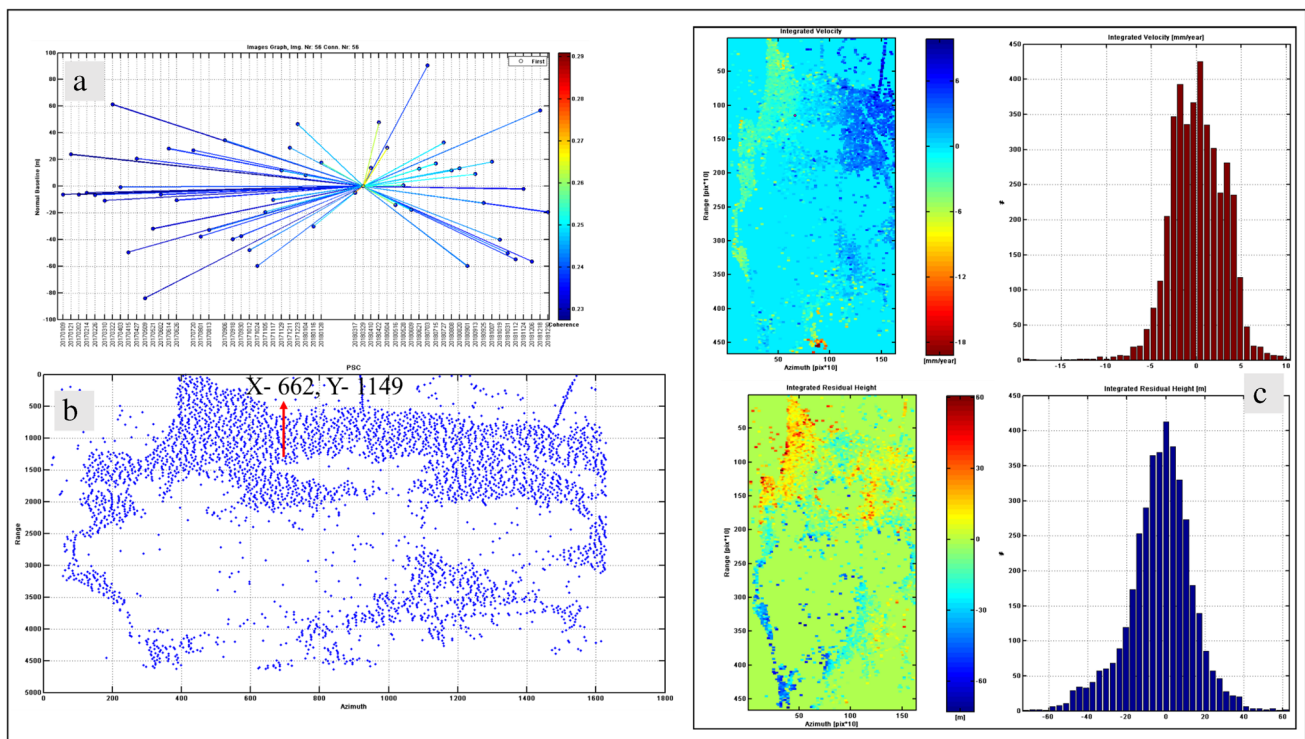
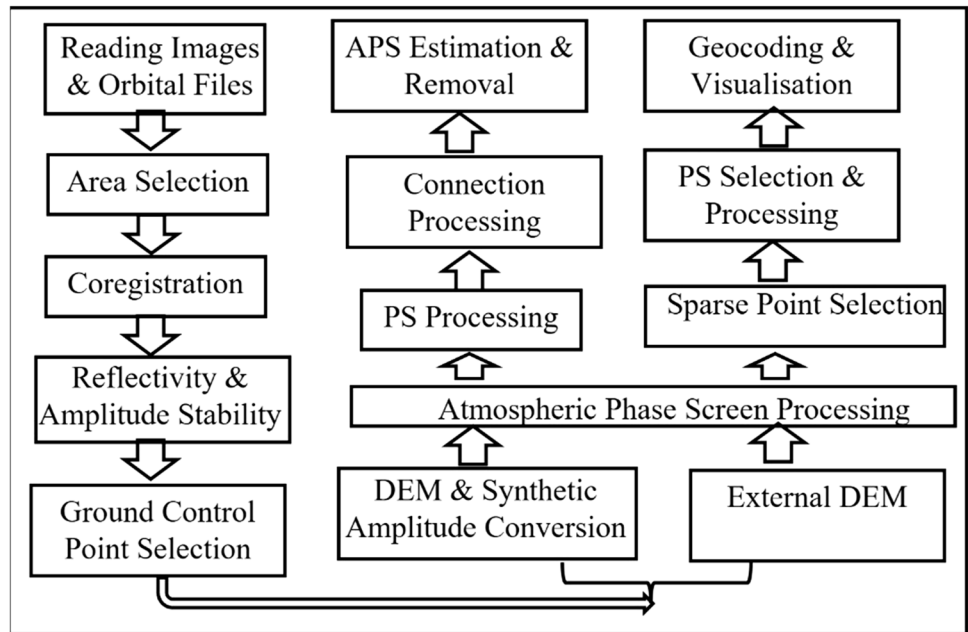
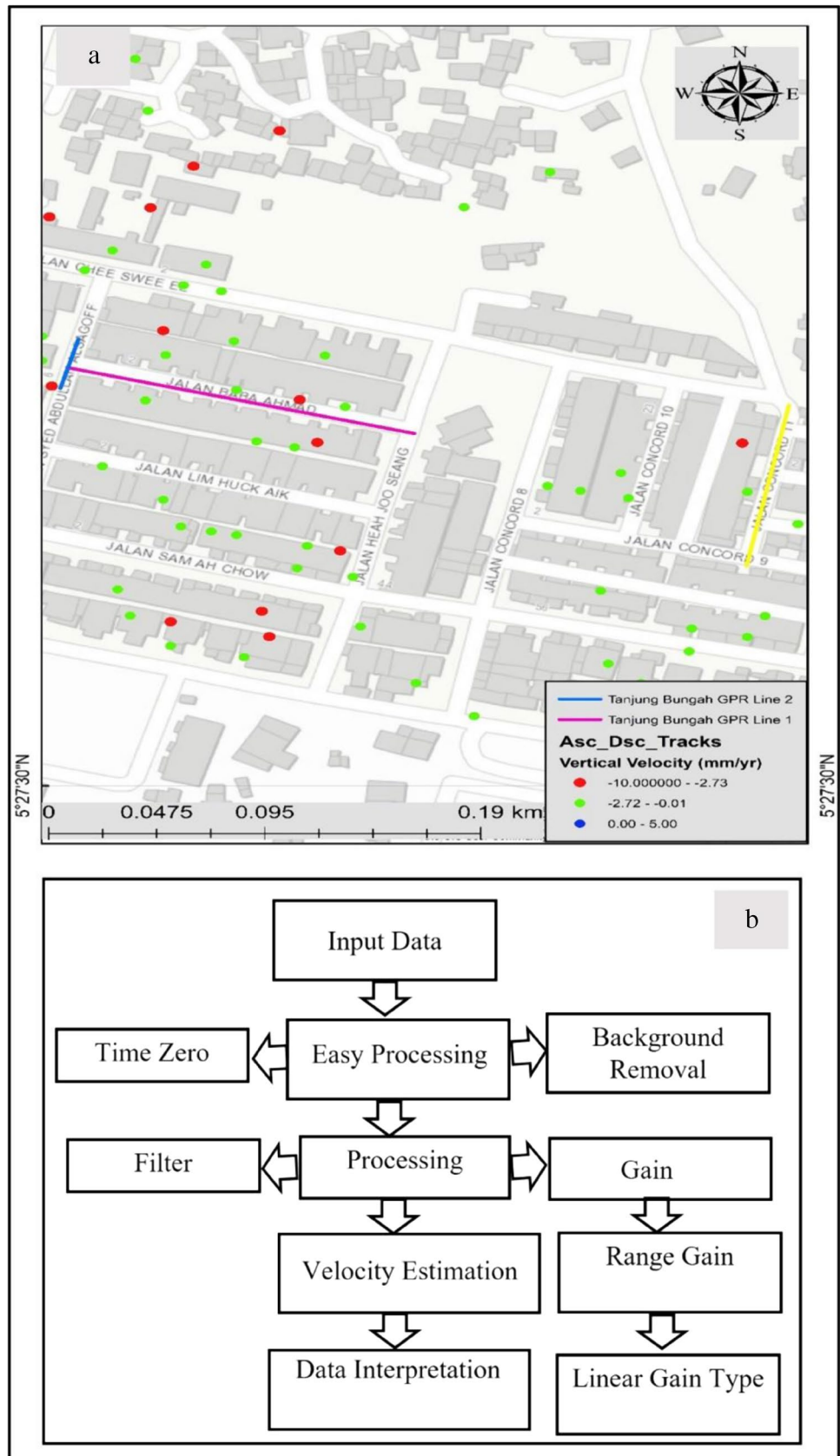


Fig. 4 The graph of Ground Control Point (GCP) (a). Traditional image graph used to connect images relating to temporal baseline (x-axis) and normal baseline (y-axis) (b). The integrated velocity and residual height (m) to zero reference point for orbit (c)

Fig. 5 GPR survey lines (after using PS technique to detect deformation areas) at Tanjung Bungah (a) and flowchart of GPR processing (b)



to intermediate microcline. The terrain comprises granite, coastal plains, and hills (Kwan et al. 1992; Pradhan and Lee 2010). The granite exhibits mineralogical and textural variations believed to have formed a discrete plutonic (North and South) complex (Cobbing et al. 1986).

Methodology

Different Synthetic Aperture Radar (SAR) satellites are designed to solve unique problems (Dogan and Perissin 2014). Sentinel 1-A (S-1A) is a radar satellite that orbits the earth and operates in the C-band (Wegmüller et al. 2016). The short revisit time makes S-1A more attractive than other SAR missions in Interferometric SAR (InSAR) applications (Haghighi and Motagh 2017). The fifty-six (56) S-1A SLC data with 5 m × 20 m resolution acquired from descending orbital geometry from 9th January 2017 to 30th December 2018, shown in Table 2, were processed by the Permanent Scatterer (PS) technique in SARPROZ software to measure

ground deformation over Penang Island. The perpendicular and temporal baselines of the acquired scenes range between – 122 to 126 and – 1693 to 792 respectively. SARPROZ software is a flexible software developed by Perissin, Purdue University, West Lafayette, IN, USA, and written in Matlab for processing InSAR data to detect the ground deformation (Perissin and Wang 2012).

Compared to other traditional measurements, such as Levelling, GPS, and Global Navigation Satellite Systems (GNSS), InSAR provides high spatial and temporal resolution surface deformation (Ferretti et al. 2001; Gama et al. 2017). PS-InSAR technique is applied to detect, analyse, and map ground deformation activities in this present work. It exploits multiple SAR images (slave) over the same region at different acquisition times, relating to one adequately chosen master (Ferretti et al. 2001). It is a versatile technique to overcome the errors introduced to the results via atmospheric conditions on the radar pulses and changes in the ground reflectivity due to differences in the ground’s vegetation or moisture content (Hung et al. 2011).

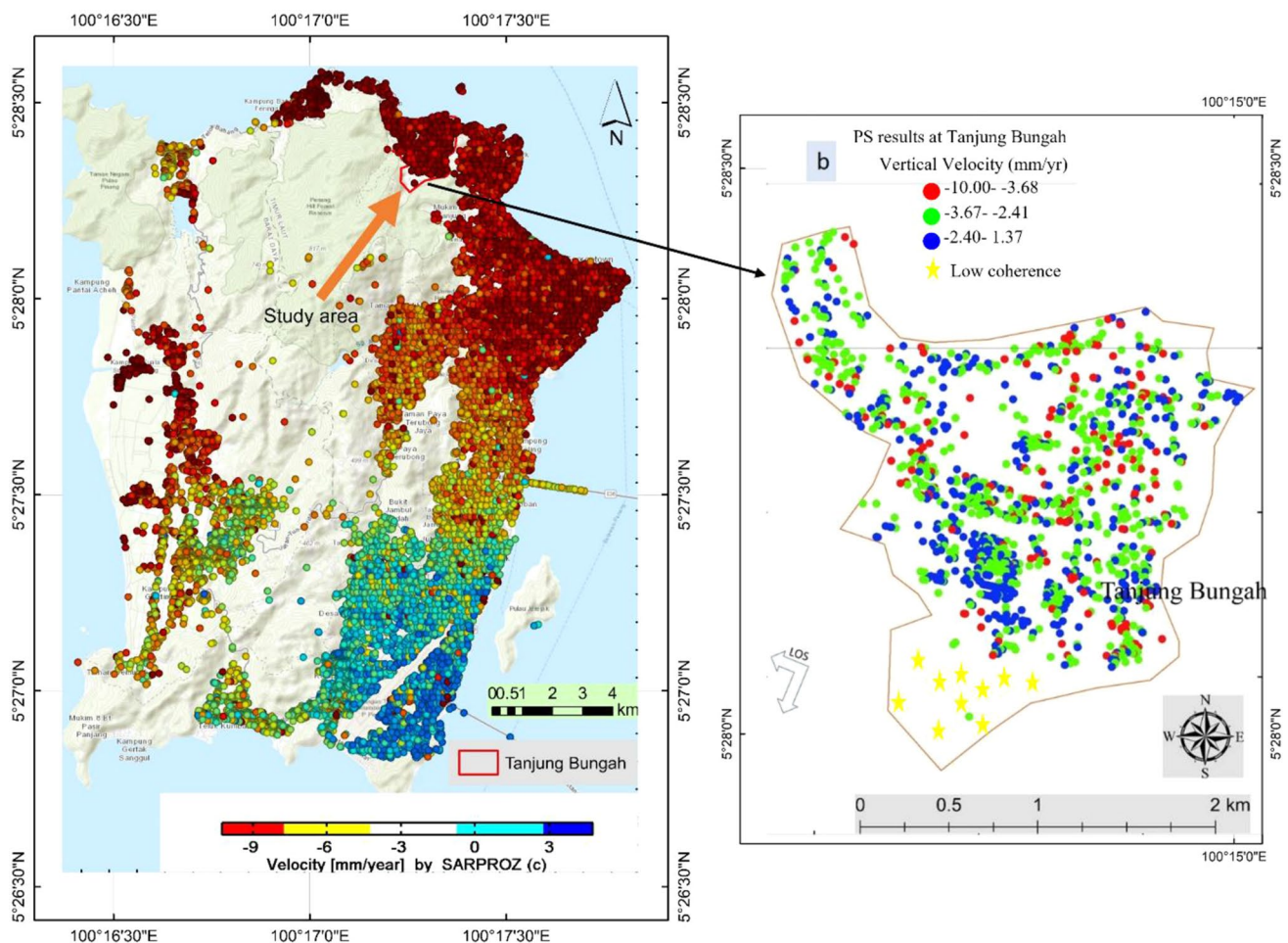


Fig. 6 PS-InSAR time series over the entire Penang Island (a) and PS-InSAR analysis of Tanjung Bungah area generated from descending Sentinel-1A IW SLC data (b)

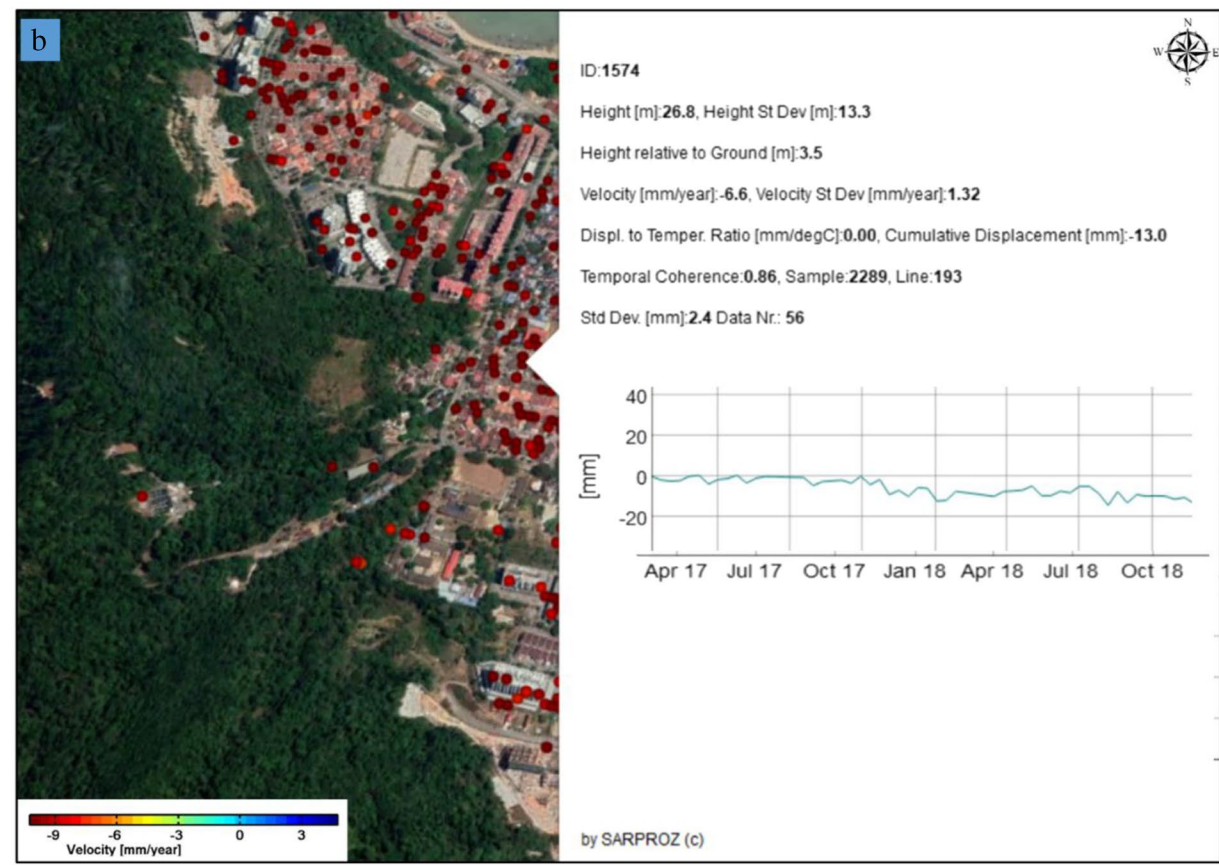
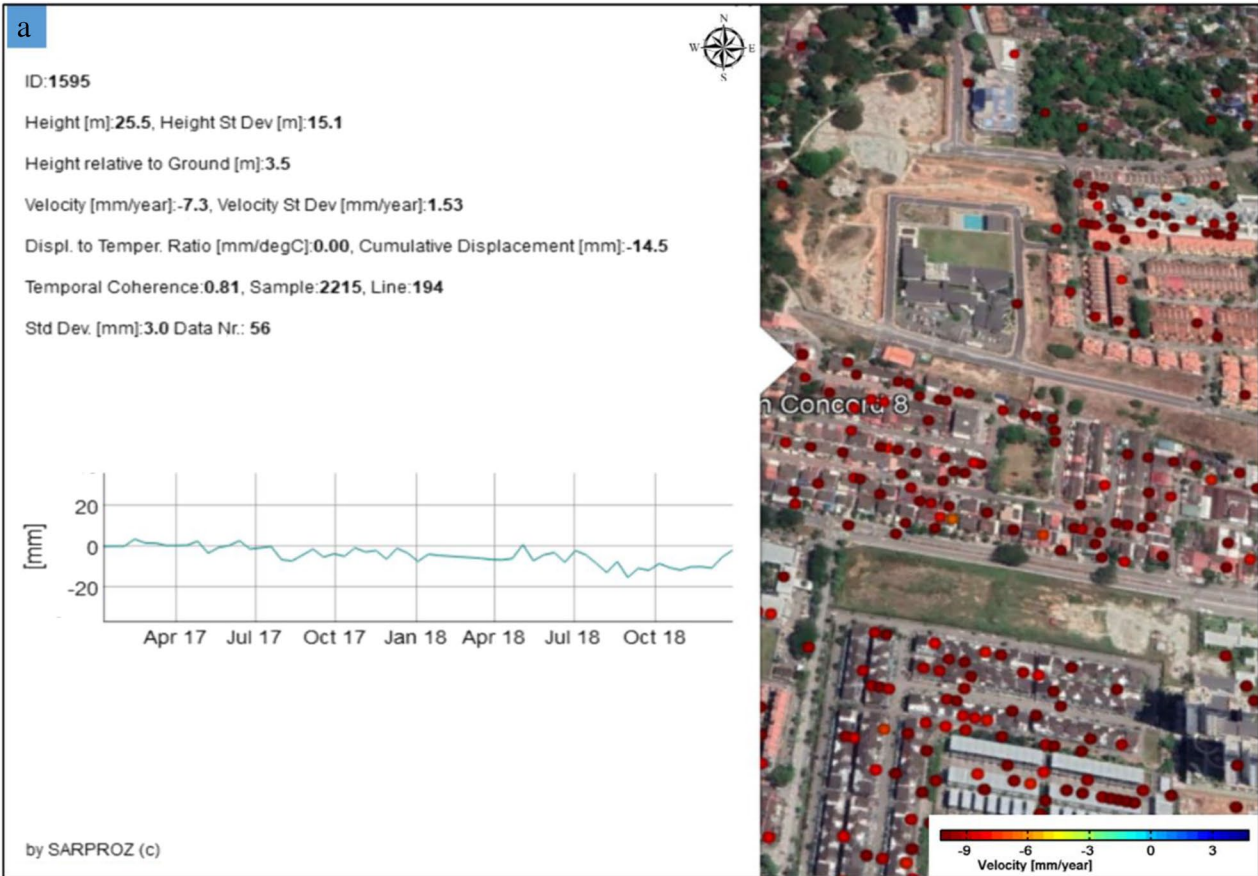


Fig. 7 Results of the PS-InSAR analysis and their respective displacement time series (in LOS) for the points at Jalan Concord (a) and Jalan Baba Ahmad (b), Tanjung Bungah

The acquired 56 SLC imageries were converted to a SARPROZ format. After importing all the images into the software, the Graphical User Interface (GUI) was used to perform various steps such as the creation of a suitable subset of the area of interest (AOI), precise orbital setting, and weather data retrieval from each scene for further processing. The software automatically populated the master scenes where a single master configuration image acquired on 29th March 2018 was selected and considered based on algorithms in the software. There was no extreme weather change on that day of acquisition.

The parameters, such as reflectivity, spatial coherence, and amplitude stability index (ASI), were considered quality estimators for PS candidates (PSCs). These are the combinations of quality parameters related to the radar signal stability of the targets. The master extraction, slave extraction, and co-registration parameters were processed, and the images were later co-registered to align all of them for comparison pixel-by-pixel without any positional errors. The atmospheric disturbances were removed using the Goldstein mode. The flow chart of the SARPROZ software is depicted in Fig. 3.

All slave images were connected to a single master image to produce interferograms. The star graph connection provides consistency of temporal baseline and enhances the ability to unwrap the phase signal to generate an accurate time series of displacement (Fig. 4a). As InSAR measures the relative motion to the reference point, a most stable reference point (at x is 662, y is 1149) as shown in Fig. 4b was selected at the maximum residual height of point zero depicted in Fig. 4c. The multi-looking (ML) factors were repeated until smooth pixels were obtained. Useful information about the deformation can easily be extracted from the generated interferograms. The results were geocoded to Google Earth and saved in a.kmz format. The quantitative data (from the PS results) were analysed using SPSS version 24.

GPR is one of the most widely used geophysical techniques for subsurface surveys, and its effectiveness depends on the site's unique conditions {Formatting Citation}. GPR survey was performed in Tanjung Bungah, Penang Island. Three (3) different GPR lines were laid at 30 m, 156 m, and 101 m length, respectively, where subsidence patterns have been detected using InSAR techniques. Before the survey, the sanitation of metallic elements on the survey sites was enacted to prevent high reflectivity elements on the surface. The configuration consists of a 300/800 MHz dual-frequency antenna, 10.8 V lithium-ion battery, an electronic unit, monitor, and a large wheel that was initially calibrated as the investigation began. The calibration was done to ensure the travel distance's accuracy, and the GPR was ensured to travel

on a straight line. The dual-frequency antenna has both the transmitter and receiver components connected to the monitor and battery. The areas were scanned by sending ultra-high-frequency electromagnetic waves into the ground from a transmitter antenna (transducer). The transmitted waves (from different submerged objects and earth materials) are reflected back to the surface as they encounter changes in the dielectric permittivity of the matrix they travel through and are detected by a receiver antenna.

RADAN 7 software of Geophysical Survey Systems, Inc. was used to perform the profile processing with the following steps: (i) Time-zero processing measures the target's depth by bringing the ground surface to zero, (ii) Background removal improves the data's transparency and eliminates any horizontal banding that might have been introduced from various sources, (iii) Filters that cut out high and low frequencies and focus on the signals needed, (iv) Gain, which jacks up the data and enhances the target, and (v) Velocity estimation that gives the chance to measure wave velocity. The flowchart of the processing steps for the GRP data is shown in Fig. 5b.

Results and discussions

The results and discussions of the Interferometric Synthetic Aperture Radar (InSAR) and geophysical survey ground-penetrating radar (GPR) are presented in this section.

PS-InSAR

Although the entire ground deformation of Penang Island was mapped using the PS technique (Fig. 6a), this paper's analyses and discussions are limited to only the region of Tanjung Bungah (Fig. 6b) where ground deformations (e.g., landslide and subsidence) have been recorded. Due to the reasonable number of processed images (> 50 images), the results gave further evaluation opportunities. A powerful module in SARPROZ software with very flexible options, i.e., "scatter plot," was used to display the ground deformation velocity results with their respective displacement time series at Tanjung Bungah, Penang Island. The lowest patterns of subsidence value of -10 mm/yr at Tanjung Bungah (Fig. 6) are observed.

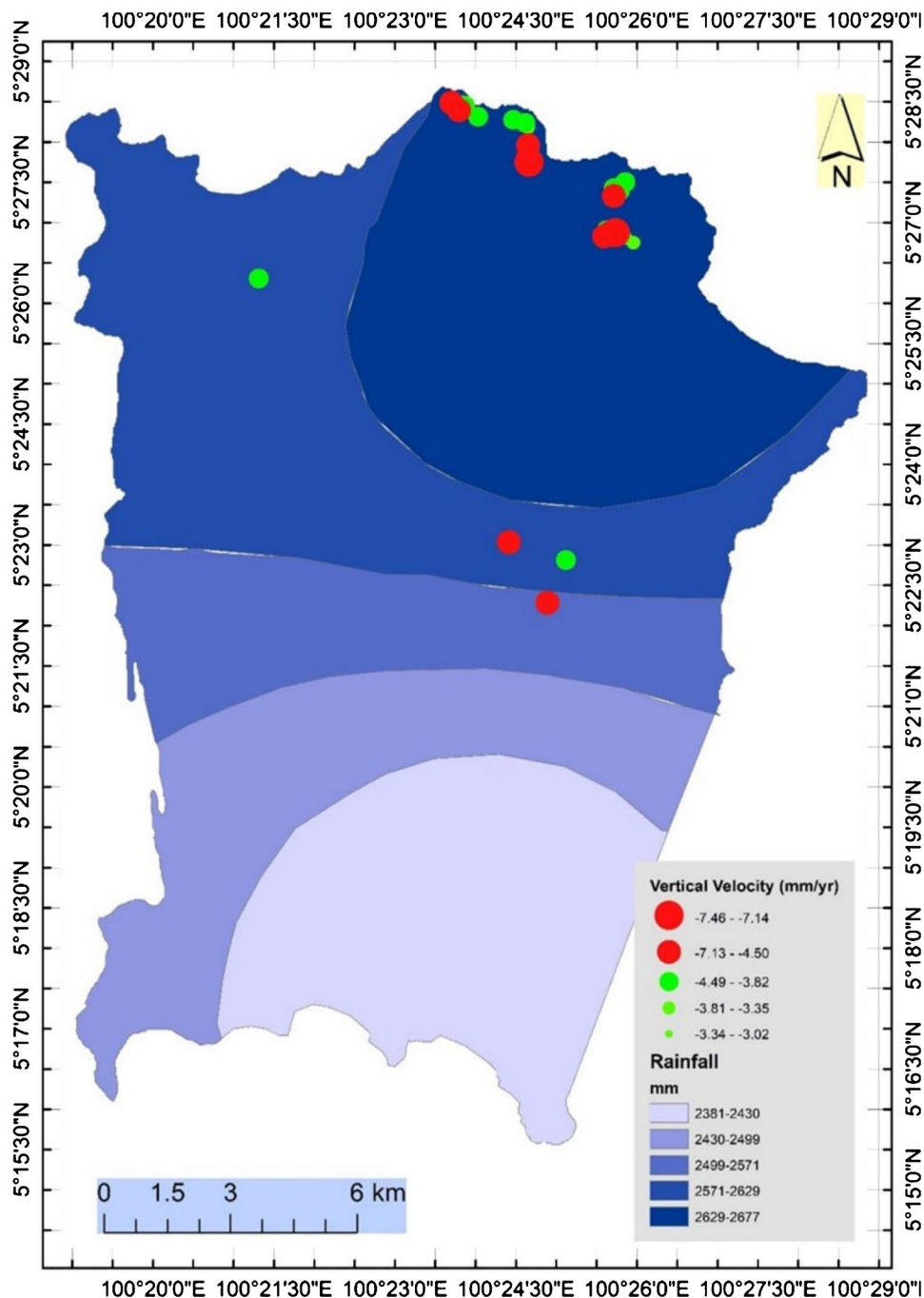
Tanjung Bungah, a geologically and historically landslide-prone area, has suffered and experienced various landslide occurrences in the past. The PS-InSAR technique was applied to process 56 descending S-1A data to detect surface deformation in the area. The positive value represents a movement (i.e., an uplift) towards the satellite. In contrast, the negative value denotes movement away from the satellite (i.e., land subsidence) along with the satellite LOS from PS measurements. The

generated deformation maps from the S-1A dataset obtained between 2017 and 2018 show the spatial distribution of land subsidence in Fig. 6. Active ground deformations were observed throughout the monitoring period, especially in low elevation areas. However, the deformations (subsidence and uplift) are distributed at different topographic locations of the studied area.

Tanjung Bungah is a landslide-prone area because of the terrain and weather conditions. Its soil area comprises clay, gravel, silt, fragile, and loose. The observed displacements shown in Fig. 7 may be due to the peak rainfall the area usually experiences between October and January. The

geological structures can also influence landslide development, formation, and acceleration. A weak structural plane is produced by the interaction between high-density bedrock and weak deposits. Therefore, external forces like rainfall and earthquake can easily slip down the plane under its gravity. The erosion of the cumulative groundwater can also break and infiltrate the clayey materials and trigger the old landslides' cracks. It is noticed that most of the landslide sites' landscape is steep at the top, moderate at the middle, and still steep at the low portion, suitable for accelerating landslides.

Fig. 8 Map of rainfall of Penang Island with subsidence values at Tanjung Bungah. The rain increases from the south to the north (modified after Khodadad and Jang, 2015)



The decreasing trend in the time series shown in Fig. 7 indicates the active site and demonstrates how the displacement magnitude increased. The soil of the study area has high water content and is vulnerable to serious hazards. The displacement graphs of the time series display the linear trend. They give better interpretations of the displacement rates in the statistical analysis. The highest magnitude of the displacement values observed correlate well with the areas where landslides are most frequent in the area.

The analyses reveal that landslide is more likely to occur when there is an increase in heavy rain's spatial extent, size, and frequency. Khodadad and Jang (2015) analysed 10 years of rainfall data of Penang Island acquired from meteorological stations between 2003 and 2012. It is reported that the rain increases from the south to the north, and the maximum rain values occur from October to January. InSAR techniques and rainfall results are found to have a linear relationship. The high values of rainfall intensity in the north correspond to the InSAR results, as shown in Fig. 8. Therefore, excessive rain is identified as one of the causes of ground displacement on Penang Island.

The methodology used needs to be validated because several parameters can affect the method's accuracy. GPS is one of the in situ measurements used to meet high accuracy standard. Ami et al. (2015) obtained GPS data from 117 stations between 1999 and 2011 to quantify Malaysia's vertical motion trend. The analyses reveal that there are vertical ground movements (uplift and subsidence) in Malaysia. The values of ground deformation vary between -0.04 and -34.41 mm/yr (subsidence) and from 0.21 to 1.44 mm/yr (uplift). The subsidence rate of -0.90 mm/yr was detected in Penang Island. This value correlates well with the values observed in this research using PS techniques at the same point. Figure 9 shows the results of Ami et. al and the InSAR results. The same value is obtained at the same point.

GPR profiles

GPR reflection mostly comes from geological structures in different depositional environments; thus, GPR is useful for

Fig. 9 Vertical displacement of GPS measurement around the study area (a) Khodadad and Jang (2015), PS points obtained at the same area by S-1A data (b)

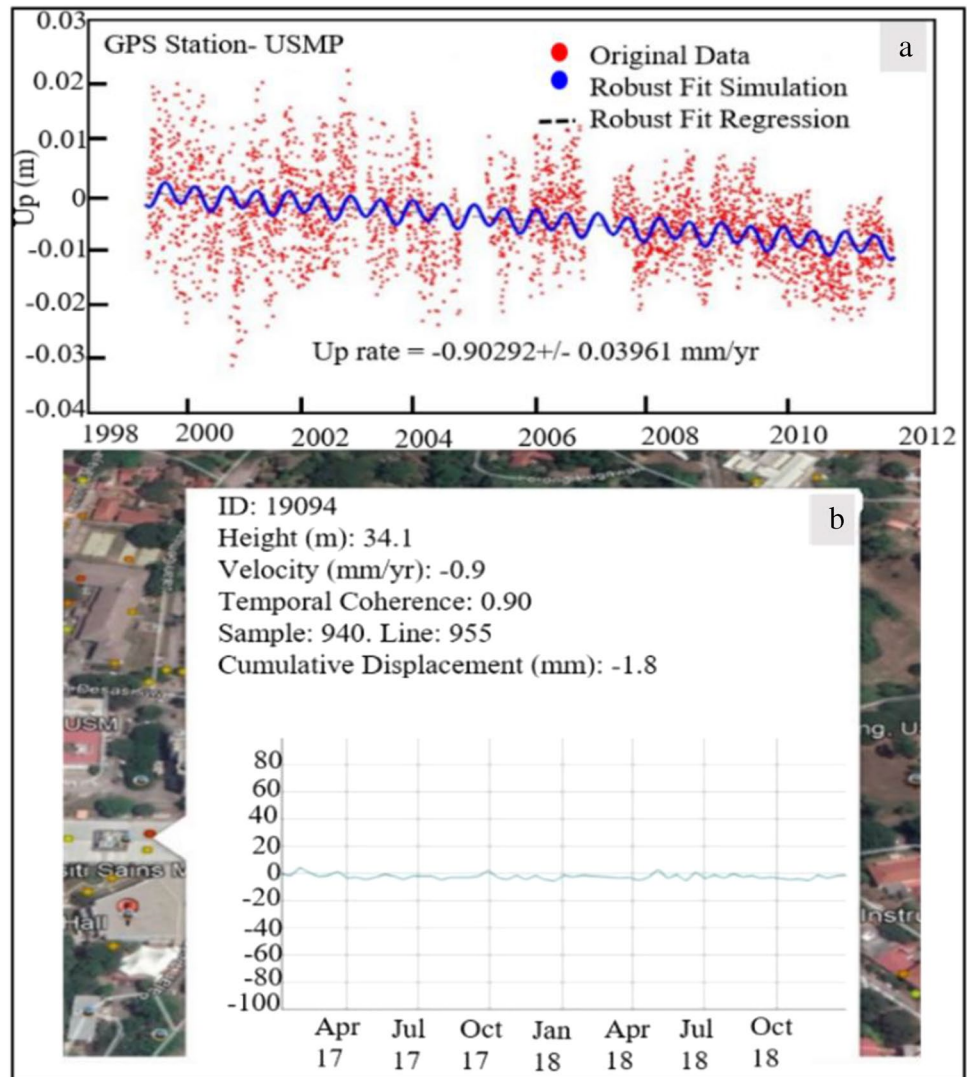
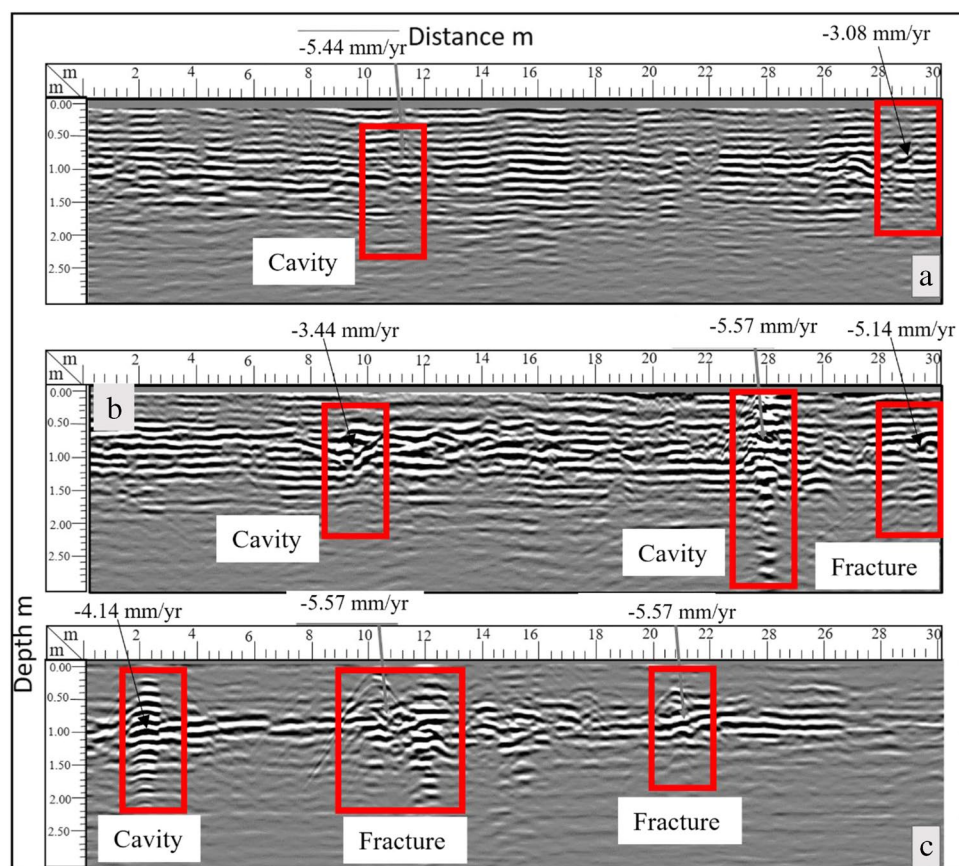


Fig. 10 Profile radargram at Tanjung Bungah Jalan Baba Ahmad (profile 1), Jalan Baba Ahmad (profile 2), and Jalan Concord



mapping lateral and vertical sediments with different materials (silt, clay, etc.). For validation and interpretation of the ground deformation, the subsidence areas detected using InSAR techniques were investigated by GPR reflection patterns (Fig. 5). The output signal peak voltages are plotted on the GPR profile by the digital control unit. The working hypothesis is that this non-intrusive geophysical method could help detect cavities at the studied site. The surveys were conducted to calibrate the appropriate depth and determine the signal's behaviour. The detected anomalies were probably associated with cavities, fractures, and road fissures.

The radargrams obtained at Jalan Baba Ahmad (TBJB) and Jalan Concord (TBJC), where different anomalies are detected, are shown in Fig. 10. At TBJB, the cavity is located at the distance of 11.64 m and 0.34-m depth from their respective starting points with -5.44 mm/yr deformation values. Anomalies are also observed at the distance of 29.16 m and 0.42-m depth with -3.08 mm/yr deformation values, as shown in Fig. 10a.

In the second survey line in TBJB (Fig. 10b), the cavities are observed at the distances and depths of 9.90 m and 0.60 m, and 27.01 m and 0.02 m, with deformation values of -3.44 and -5.57 and respectively. Fractures are observed at the distance of 29.40 m and 0.60-m depth from their starting point with the deformation value of -5.17 mm/yr.

At TBJC (Fig. 10c), the cavity is noticed at the distance of 2.10 m and 0.22-m depth from their starting points with deformation values of -4.14 mm/yr.

Two road fractures located at the distance of 9.78 m and 0.35-m depth and at the distance of 26.70 m and 1.10-m depth from the starting points with their respective deformation values of $-0.5.57$ mm/yr were also observed. Different approaches were introduced to gain useful information about the ground deformations from the studied sites. The perpendicular and parallel approaches are used at Tanjung Bungah (Fig. 5a). The entire series of ground deformations of the studied areas are characterised by high water and sand content, which increase with depth.

Conclusion

The PS-InSAR technique, a dynamic technique for detecting and measuring ground deformation activities, has been used to map and quantify Tanjung Bungah deformations. The results reveal that the PS-InSAR is an excellent technique for mapping surface deformations in the study area as significant deformations of -10.00 mm/yr (subsidence) and 5.00 mm/yr

(uplift) were detected in the direction of LOS. Some landslide locations have been recognised in the analyses.

The GPR method was used to image the distribution of deformation structures and subsidence behaviour at a shallow depth of the study area. Anomalies that corresponded to cavities and fractures located at different depths were detected. The results show that GPR is a suitable geophysical tool to identify and map subsurface cavities. The combination of PS-InSAR and GPR gave a better understanding and interpretation of the results and proved their usability in the study. It is obvious that one single approach cannot be used as a stand-alone tool for solving landslide challenges in an urban area. InSAR is used to explore broad areas, detect deformation, and investigate spatio-temporal evolution. The geophysical process enables the geometry of near-surface geological structures with a high spatial resolution at a low cost to be characterised.

Acknowledgements The authors would like to thank the European Space Agency (ESA) for making Sentinel-1A data available free of charge.

Funding Universiti Sains Malaysia and Tertiary Education Trust Fund (TETFUND), Nigeria are equally acknowledged for supporting this research.

Declarations

Conflict of interest The authors declare no competing interests.

References

- Ahmad F, Yahaya AS, Halim MH, Sian KC (2014) Analysis of thickness of sand and silt in Penang Island. *J Civ Eng Res* 4:41–47
- Ali MM, Ahmad F, Yahaya AS, Farooqi MA (2011) Characterisation and hazard study of two areas of penang Island, Malaysia. *Hum Ecol Risk Assess* 17:915–922
- Ami HMD, Mohd Nadzri MR, Kamaludin MO, Sahrum S, Amir SAL (2015) Monitoring vertical land motion in Malaysia using global positioning system (GPS). *Proceeding of the 36th Asian Conference on Remote Sensing (ACRS)* (Metro Manila, Philippines, 19–23 October)
- Bayer B, Simoni A, Schmidt D, Bertello L (2017) Using advanced InSAR techniques to monitor landslide deformations induced by tunneling in the Northern Apennines, Italy. *Eng Geol* 226:20–32
- Chacko RP (2019) Sliding down the slippery slopes of unsustainability: rampant hill development in Penang. *Heintich Boll Stiff Southeast Asia* 1–9
- Choi J-K, Kim K-D, Saro Lee JW (2010) Application of a fuzzy operator to susceptibility estimations of coal mine subsidence in Taebaek City, Korea. *Env Earth Sci* 59:1009–1022
- Cobbing EJ, Mallick DIJ, Pitfield PEJ, Teoh LH (1986) The granites of the southeast Asian tin belt. *J Geol Soc London* 143:537–550
- Dogan O, Perissin D (2014) Detection of multitransition abrupt changes in multitemporal SAR images. *IEEE J Sel Top Appl Earth Obs Remote Sens* 7:3239–3247
- Ferretti A, Prati C, Rocca F (2001) Permanent scatterers in SAR interferometry. *IEEE Trans Geosci Remote Sens* 39:8–20
- Galve JP, Cevalco A, Brandolini P, Soldati M (2015) Assessment of shallow landslide risk mitigation measures based on land use planning through probabilistic modelling. *Landslides* 12:101–114
- Gama FF, Cantone A, Mura JC, Pasquali P, Paradella WR, dos Santos AR, Silva GG (2017) Monitoring subsidence of open pit iron mines at Carajás Province based on SBAS interferometric technique using TerraSAR-X data. *Remote Sens Appl Soc Environ* 8:199–211
- Gazzaz NM, Yusoff MK, Aris AZ, Juahir H, Ramli MF (2012) Artificial neural network modeling of the water quality index for Kinta River (Malaysia) using water quality variables as predictors. *Mar Pollut Bull* 64:2409–2420
- Guzzetti F, Carrara A, Cardinali M, Reichenbach P (1999) Landslide hazard evaluation: a review of current techniques and their application in a multi-scale study, Central Italy. *Geomorphology* 31:181–216
- Haghighi MH, Motagh M (2017) Sentinel-1 InSAR over Germany: large-scale interferometry, atmospheric effects, and ground deformation mapping. *ZfV - Zeitschrift Fur Geodasie, Geoinf Und Landmanagement* 142:245–256
- Huang J, Khan SD, Van Nieuwenhuise D, Khan AS (2020) Reflection seismic, gravity, magnetic, and InSAR analysis of the Chaman Fault in Pakistan. *Arab J Geosci* 13:576
- Hung WC, Hwang C, Chen YA, Chang CP, Yen JY, Hooper A, Yang CY (2011) Surface deformation from persistent scatterers SAR interferometry and fusion with leveling data: a case study over the Choushui River Alluvial Fan. *Taiwan Remote Sens Environ* 115:957–967
- Kavzoglu T, Sahin EK, Colkesen I (2014) Landslide susceptibility mapping using GIS-based multi-criteria decision analysis, support vector machines, and logistic regression. *Landslides* 11:425–439
- Khodadad S, Jang D (2015) A comparative study of analytical hierarchy process and ordinary least square methods for landslide susceptibility mapping using GIS technology. *Tojsat* 5:7–16
- Kwan TS, Krähenbühl R, Jäger E (1992) Rb-Sr, K-Ar and fission track ages for granites from Penang Island, West Malaysia: an interpretation model for Rb-Sr whole-rock and for actual and experimental mica data. *Contrib to Mineral Petrol* 111:527–542
- Lee S, Pradhan B (2006) Probabilistic landslide hazards and risk mapping on Penang Island, Malaysia. *J Earth Syst Sci* 115:661–672. <https://doi.org/10.1007/s12040-006-0004-0>
- Oh HJ, Pradhan B (2011) Application of a neuro-fuzzy model to landslide-susceptibility mapping for shallow landslides in a tropical hilly area. *Comput Geosci* 37:1264–1276
- Perissin D, Wang T (2012) Repeat-pass SAR interferometry with partially coherent targets. *IEEE Trans Geosci Remote Sens* 50:271–280
- Pradhan B, Lee S (2010) Delineation of landslide hazard areas on Penang Island, Malaysia, by using frequency ratio, logistic regression, and artificial neural network models. *Environ Earth Sci* 60:1037–1054
- Pradhan B, Chaudhari A, Adinarayana J, Buchroithner MF (2012) Soil erosion assessment and its correlation with landslide events using remote sensing data and GIS: a case study at Penang Island, Malaysia. *Environ Monit Assess* 184:715–727
- Pradhan B, Abokharima MH, Jebur MN, Tehrany MS (2014) Land subsidence susceptibility mapping at Kinta Valley (Malaysia) using the evidential belief function model in GIS. *Nat Hazards* 73:1019–1042
- Rauff KO, Abir IA, Perissin D (2020) Characterisation of landslide using InSAR technique and electrical resistivity method at Paya Terubong, Malaysia. *J Indian Soc Remote Sens* 48(8):1223–1236

- Rocca F, Prati C, Ferretti A, Colesanti C, Novali F (2003) Sar monitoring of progressive and seasonal ground deformation using the permanent scatterers technique. *IEEE Trans Geosci Remote Sens* 41:1685–1701
- Rocca A, Mazzanti P, Perissin D, Bozzano F (2014) Detection of past slope activity in a desert area using multi-temporal DInSAR with ALOS PALSAR data. *Ital J Eng Geol Environ* 1:35–50
- Tan BK (1994) Engineering properties of granitic soils and rocks of Penang Island, Malaysia. *Bull Geol Soc Malaysia* 35:69–77
- Tan KC, Lim HS, MatJafri MZ, Abdullah K (2010) Landsat data to evaluate urban expansion and determine land use/land cover changes in Penang Island, Malaysia. *Environ Earth Sci* 60:1509–1521
- Thuro K, Singer J, Festl J, Wunderlich T, Wasmeier P, Reith C, Heu-neckel O, Glabsch J, Schuhbäck S (2010) New landslide monitoring techniques—developments and experiences of the alpEWAS project. *J Appl Geod* 4:69–90
- Tofani V, Raspini F, Catani F, Casagli N (2013) Persistent scatterer interferometry (PSI) technique for landslide characterisation and monitoring. *Landslide Sci a Safer Geoenvironment Vol 2 Methods Landslide Stud* 5:1045–1065
- Tymchenko O, Ugnenko E, Makovyey R (2016) Analysis of methods of landslide processes forecasting on highways. *Procedia Eng* 134:146–152
- Van Westen CJ (2000) The modeling of landslide hazards using GIS. *Surv Geophys* 21:241–255
- Wegnüller U, Werner C, Strozzi T, Wiesmann A, Frey O, Santoro M (2016) Sentinel-1 support in the GAMMA software. *Procedia Comput Sci* 100:1305–1312

Springer Nature or its licensor holds exclusive rights to this article under a publishing agreement with the author(s) or other rightsholder(s); author self-archiving of the accepted manuscript version of this article is solely governed by the terms of such publishing agreement and applicable law.